1.9 picosecond high-sensitivity sampling optical temporal analyzer

Yi Chen,[a] Steve Williamson,[b] and Tim Brock
Ultrafast Science Laboratory, University of Michigan, Ann Arbor, Michigan 48109-2099

An all solid-state, high-sensitivity sampling optical temporal analyzer has been demonstrated by integrating two interdigitated picosecond metal-semiconductor-metal photodetectors into a coplanar transmission line structure. The full width at half-maximum of the response time is 1.9 ps. The noise equivalent optical power is 500 pW, and the dynamic range is more than 60 dB.

The rapid development of ultrafast sciences places an increasing demand on high-speed, high-dynamic range measurement techniques. An optical correlation technique based on photoconductivity for measuring ultrafast laser pulses was first demonstrated by Austin et al.[1] However, due to relatively low efficiency of both signal detection and sampling, such a system was not able to measure weak optical signals. Recently, Li et al.[2] showed that a Schottky photodiode with the integration of a microwave detector can measure weak optical laser pulses with picosecond resolution. In this letter, we report an all solid-state circuit that we believe is the best in terms of speed and dynamic range for performing optical correlation measurements. Our device structure is based on Ketchen et al.'s[3] original work with incorporation of a high-speed, high-responsivity metal-semiconductor-metal (MSM) interdigitated photodetector/switch developed in our laboratory. As the result, we obtained a novel sampling optical temporal analyzer (SOTA) with high sensitivity. We were able to measure extremely weak signals with picosecond resolution.

We reported earlier[4] that an interdigitated MSM photoconductive detector grown on low-temperature (LT) GaAs can function as either a high-sensitivity photodetector or photoswitch. As a detector, operating at a low input optical power level of 4 μW (0.04 pJ/pulse), the device has a response time of 1.2 ps and responsivity of 0.1 A/W. As input optical power level increases to >1 mW (10 pJ/pulse), the same device functions as high-sensitivity photoconductive switch. With an input power of 2.2 mW (22 pJ/pulse), the gap resistance is driven from 10^7 to 30 Ω, while the time resolution increases to only 1.5 ps. Our experiment takes advantage of this unique functionality for picosecond measurement of low-intensity optical signals.

Figure 1 shows the schematic diagram of the SOTA experiment. The interdigitated structure bridging between the coplanar transmission lines functions as the photodetector. We placed interdigitated detector between coplanar transmission lines instead of using photoconductive gap switching to assure good coupling of the generated electrical pulse to the propagating mode. The second interdigitated structure, connected between the ground electrode of the transmission lines and the sampling line, functions as photoswitch to sample the signal. The separation between the photodetector and the photoswitch is 100 μm in our case. The detector and switch are identical. The finger width and spacing are 0.2 μm. The active area is 7 μm $\times$8 μm. The coplanar transmission lines have a strip width of 20 μm and a separation of 20 μm. The characteristic impedance is 90 Ω. The entire structure was fabricated on LT-GaAs. The LT-GaAs layer was grown on a (100) semi-insulating GaAs substrate which has a 0.4-μm conventionally grown undoped buffer layer. The LT-GaAs layer was grown to a thickness of 1.5 μm at a substrate temperature of 190 °C and subsequently annealed at 600 °C for 10 min in an arsenic overpressure. The interdigitated electrodes are fabricated of 300 Å/2000 Å Ti/Au using a JEOL JBX 5DIIF direct-write e-beam lithography system. Coplanar transmission line electrodes of 20-μm spacing/width and 5-mm length are also fabricated of 500 Å/2500 Å Ti/Au using conventional optical lithography. No antireflection coating is placed over either the photodetector or the photoswitch in this initial work.

We use the photoconductive sampling technique to characterize the SOTA. A balanced, colliding pulse, mode-locked dye laser operating at 610 nm with a repetition rate of 100 MHz produces 150 fs pulses. We use 150 fs optical pulses for both the signal under study and the gate pulse. As shown in Fig. 1, the pump beam is focused onto the interdigitated photodetector and its average power adjusted from 4 mW to 1 nW using a variable attenuator. The detector is dc-biased through the coplanar transmission lines. An electrical pulse is switched into the transmission lines as the femtosecond pump optical pulse hits the interdigitated photodetector. The signal is sampled at the photoconductive gate as the gate pulse turns on the photoswitch. The gate pulse typically has a power of 3 mW (30 pJ/pulse). The current obtained at the sampling gate is amplified by a current amplifier.

Figure 2 shows the temporal response of the SOTA. A set of wave forms are measured at different input optical power levels. Each curve represents almost three orders of magnitude difference in average optical power. The highest power is 4 mW (40 pJ/pulse), the lowest power being 8 nW (80×10^{-6} pJ/pulse), spanning almost six orders of magnitude. The dc bias on this 0.2 μm interdigitated detector is 4 V. The dramatic change in pulse energy shows virtually no degradation in the response of the SOTA. The full width at half-maximum for input optical power of 4 μW is 1.9 ps, matching the convolution value of 1.9 ps for detector (1.2 ps) and gate (1.5 ps) responses. The response of the SOTA for 4 mW input power is slightly slower due to the slower re-

---

[a]Current address: AT&T Bell Laboratories, Rm. 4H616, 101 Crawfords Corner Road, Holmdel, NJ 07733-3030.
[b]Current address: Picotronix Inc., P.O. Box 130243, Ann Arbor, MI 48113-0243.
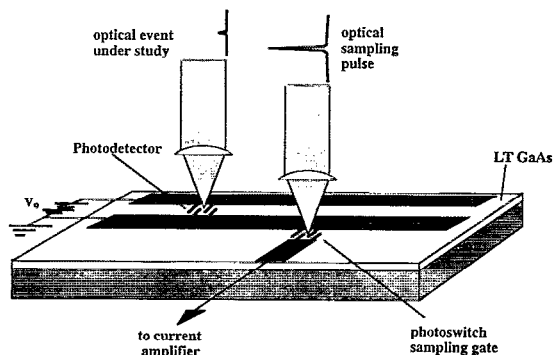
FIG. 1. Schematic diagram of the SOTA experiment.

sponse of the interdigitated photodetector at high input power levels.[4] As input power decreases to 8 nW, the signal-to-noise ratio is still 5:1 with an integration time of 100 ms. This corresponds to a noise equivalent power (NEP) of 500 pW for the SOTA, or 16 photons/pulse at 100 MHz repetition rate. The dynamic range is more than 60 dB.

For comparison, we performed an experiment without the interdigitated photodetector and photoswitch in place. Such a measurement is essentially a conventional photoconductive sampling with 20-μm gap photoconductive switch and 20-μm gap photoconductive gate. Figure 3 shows the response for both conventional photoconductive sampling and the SOTA measurement. The input power for the conventional photoconductive sampling is 0.8 mW, and the input power the SOTA is only 0.1 μW. However, the signal-to-noise ratio is approximately equal for such dramatic change in input power level. This indicates that the SOTA is capable of detecting an optical signal 8000 times weaker. The 8000 times increase in sensitivity for the SOTA is the result of increased sensitivity of both detector and gate by using interdigitated structures. The switched peak voltage V_{out} on the transmission lines is given by[5]

$$V_{out} = V_{dc}[Z_0/(R_s + Z_0)], \tag{1}$$

where V_{dc} is the dc bias on the transmission lines, Z_0 is the

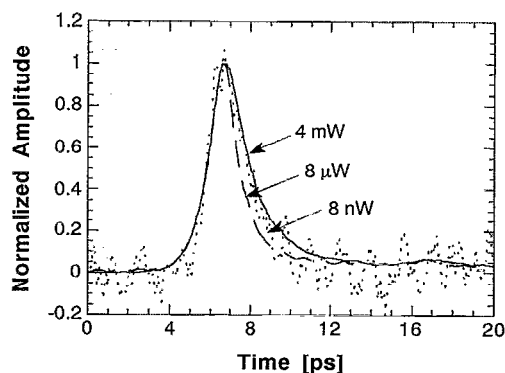
FIG. 2. Temporal response of the SOTA for different input power levels. The three curves in the figure represent the input power levels of 4 mW, 8 μW, and 8 nW, respectively, spanning almost six orders of magnitude.
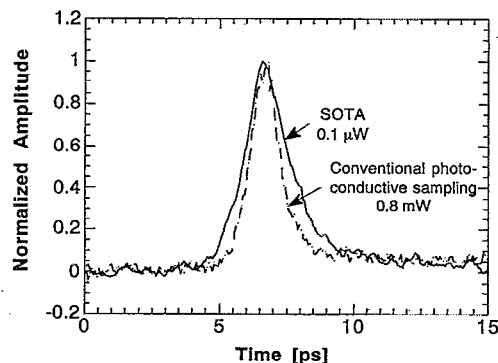

FIG. 3. Temporal response of the SOTA compared with a conventional photoconductive (PC) gap sampling. The two curves have approximately equal signal-to-noise ratio, though their input signals differ by a factor of 8000.

characteristic impedance of the transmission lines, and R_s is the on-state resistance of the photoconductive gap. The on-state resistance for a 20-μm photoconductive gap is 5 kΩ as measured directly from electro-optic sampling.[6] The on-state resistance of the interdigitated photodetector is only 30 Ω for the same power level.[4] If we assume every other condition is the same, the switched voltage for the SOTA at the detector end is 41 times higher than that of a simple coplanar transmission line switching as obtained from Eq. (1). At the gate, the switched current to current amplifier is at least 166 higher for the SOTA as a result of 166 reduction in photoconductive gate resistance. The combinational gain in sensitivity is at least 41×166, or 6833. This is very close to what we obtained in the experiment. We also notice in Fig. 3 that the response of the conventional photoconductive sampling is faster than that of the SOTA response. This is the result of finite capacitance of the interdigitated structures of the SOTA system.

We now analyze the noise sources that limit the NEP of the SOTA. There are noise contributions from both photodetector and photoswitch of the SOTA. The dominant noise currents are shot, i_{shot}, and thermal noise current, $i_{thermal}$, given by the following equations,[7] respectively:

$$i_{shot} = \sqrt{2q(I_P + I_D)}(A/\sqrt{Hz}), \tag{2}$$

$$i_{thermal} = \sqrt{4kTG}(A/\sqrt{Hz}), \tag{3}$$

where q is the electron charge, I_P is the average signal current, I_D is the dark current, k is the Boltzmann constant, T is the temperature, and G is the average conductance of the gate. At the detector, the average photocurrent I_P is 2.5×10^{-11} A with 500 pW average optical power, obtained from 0.1 A/W responsivity and taking into account of current going two directions. The dark current is 400 nA in this case. The average thermal conductance is 10 MΩ, obtained by the bias divided by the total average current. Using these parameters, we obtain $i_{shot} = 1 \times 10^{-15}$ A/Hz$^{1/2}$ and $i_{thermal} = 4 \times 10^{-14}$ A/Hz$^{1/2}$ from Eqs. (2) and (3), respectively, for the photodetector. The average photocurrent is several orders of magnitude above both the shot and thermal noise floor at the detector end. The measured signal current I_P at photoconductive switch is 3.2×10^{-13} A as obtained from

Chen, Williamson, and Brock

current amplifier. The dark current is negligible. We calculate $i_{shot} = 3.1 \times 10^{-16}$ A from Eq. (2). The off-state resistance is 10 MΩ and on-state resistance is 30 Ω at the photogate. With a duty cycle of 1.5×10^{-4} (1.5 ps gate open time versus 10 ns pulse repetition rate), this gives an average conductance of 5.1×10^{-6} mhos. The correspondent thermal noise is 2.9×10^{-13} A/Hz$^{1/2}$ as calculated from Eq. (3), far more dominant than shot noise at the gate. The thermal noise current amplitude is close to the signal current at gate. We conclude that the NEP of the SOTA system is limited by thermal noise at gate. We notice that only 1/80 of the signal current on the transmission lines is switched to the current amplifier, even though the gate resistance at on state is lower than the transmission line impedance. At present, it is not completely clear to us what is limiting the switching efficiency of the gate.

In conclusion, we have demonstrated a sampling optical temporal analyzer with the integration of two interdigitated structures on coplanar transmission lines. The SOTA is able to measure extremely low optical signals with picosecond resolution and high dynamic range. The photoconductive sampling nature of the SOTA makes it also an effective tool for timing multiple optical events at picosecond resolution.

This enables us to perform ultraweak fluorescence and scattering experiments as well as optical ranging experiments that occur on the picosecond time scale.

[1] D. H. Austin, Appl. Phys. Lett. 26, 102 (1975).

[2] K. D. Li, A. S. Hou, E. Ozbay, B. A. Auld, and D. M. Bloom, Appl. Phys. Lett. 61, 3104 (1992).

[3] M. B. Ketchen, D. Grischkowsky, T. C. Chen, C. C. Chi, I. N. Duling, N. J. Halas, J.-M. Halbout, J. A. Kash, and G. P. Li, Appl. Phys. Lett. 48, 753 (1986).

[4] Yi Chen, Steve Williamson, Tim Brock, F. W. Smith, and A. R. Calawa, Appl. Phys. Lett. 59, 1984 (1991).

[5] W. C. Nunnally and R. B. Hammond, Picosecond Optoelectronics Devices, edited by C. H. Lee (Academic, Orlando, Florida, 1984), p. 373–398.

[6] M. Y. Frankel, J. F. Whitaker, G. A. Mourou, F. W. Smith, A. R. Calawa, IEEE Trans. Electron Devices ED-37, 2493 (1990).

[7] S. M. Sze, Physics of Semiconductor Devices, 2nd ed. (Wiley, New York, 1981), p. 111.